Magnetic properties of the reentrant ferromagnetic superconductor $HoMo_6S_8$

J. W. Lynn
Department of Physics and Institute for Physical Science and Technology, University of Maryland, College Park, Maryland 20742

G. Shirane and W. Thomlinson
Department of Physics, Brookhaven National Laboratory, Upton, New York 11973

R. N. Shelton
Ames Laboratory—U.S. Department of Energy and Department of Physics, Iowa State University, Ames, Iowa 50011

D. E. Moncton
Bell Laboratories, Murray Hill, New Jersey 07974

(Received 27 February 1981)

Neutron diffraction and ac susceptibility techniques have been used to study the magnetic and superconducting phase transitions in the ternary Chevrel phase system $HoMo_6S_8$. The material first becomes superconducting at $T_{c1}=1.82$ K. With further decrease of temperature ferromagnetic correlations develop, with a correlation range in real space which increases with decreasing temperature. On further cooling, a long-wavelength (~ 230 Å) oscillatory magnetic state forms ($T_{os}=0.71$ K) in the superconducting phase, with a wavelength which increases with the application of a magnetic field. At still lower temperatures the superconductivity is destroyed ($T_{c2}^{(C)}=0.612$ K) as long-range ferromagnetic order sets in. The ferromagnetic phase at low temperatures is characterized by a saturated magnetic moment $\mu_z=9.06\pm0.3\ \mu_B$, with the spins directed along the unique [111] trigonal axis. When the material is warmed from the ferromagnetic state, no oscillatory magnetic phase appears to form, with the system passing directly from ferromagnetism to superconductivity at $T_{c2}^{(W)}=0.668$ K.

I. INTRODUCTION

The possible coexistence of long-range magnetic order and superconductivity on a microscopic scale has been an intriguing and at times controversial subject since the discovery of the $(Ce_{1-x}R_x)Ru_2$ (R a rare earth) system, where it was found that rather large concentrations of heavy rare-earth ions could be accommodated in the lattice substitutionally without adversely affecting the superconducting properties.[1–3] These substitutional alloys, however, undergo a ferromagnetic-cluster spin freezing at low temperatures rather than a conventional transition to long-range ferromagnetic order.[4–6] The subject has received renewed attention with the discovery of ternary superconducting compounds in which the magnetic rare-earth ions reside on a periodic lattice.[7,8] For all of these materials the localized $4f$ electrons have only a small interaction with the superconducting electrons, leading to a weak spin-depairing mechanism[9] as well as low magnetic transition temperatures. If the ordering is antiferromagnetic, the superconductivity is preserved so that there is true coexistence.[10] If the interactions are ferromagnetic, however, the associated dipolar field is strongly competitive with the superconducting state. We find that for $HoMo_6S_8$ a conventional uniform ferromagnetic state does not coexist with superconductivity, but rather an oscillatory magnetization first forms in the superconducting phase. As the magnetic state continues to develop with decreasing temperature, the preference for ferromagnetic alignment eventually dominates energetically and the sample is driven back to the normal conducting state.

In the following section we will discuss the basic ferromagnetic phase transition and the magnetic properties at low temperatures. We will then provide a detailed examination of the reentrant transition and the interplay between the ferromagnetic and superconducting states. We will compare the behavior of $HoMo_6S_8$ with some of the theoretical expectations and with the behavior observed in the related ferromagnetic-superconducting system $ErRh_4B_4$, where the effects of the interaction between ferromagnetism and superconductivity have also been observed recently.[11] Finally we will briefly remark on the behavior observed in the other ferromagnetic superconductors $ErRh_{1.1}Sn_{3.6}$ and $(Ce_{1-x}R_x)Ru_2$. Some portions of our work on $HoMo_6S_8$ have been briefly reported in the literature previously.[12,13]

TABLE I. Lattice parameters and superconducting transition temperatures for our $HoMo_6S_8$ sample.

$T=1.30$ K (neutrons)	$a=(6.427\pm0.003)$ Å	$\alpha=(89.31\pm0.04)^\circ$
$T=295$ K (x rays and neutrons)	$a=(6.458\pm0.004)$ Å	$\alpha=(89.52\pm0.06)^\circ$
T_{c1}	Center at 1.82 K;	Width: (1.894 → 1.754)
T_{c2} (cooling)	Center at 0.612 K;	Width: (0.646 → 0.577)
T_{c2} (warming)	Center at 0.668 K;	Width: (0.692 → 0.634)

II. SAMPLE PROPERTIES AND EXPERIMENTAL PROCEDURES

A polycrystalline sample weighing about 4 g was prepared by powder metallurgy. Binary compounds of HoS and $Mo_{2.06}S_3$ (Ref. 14) were synthesized from high-purity elements including H_2-reduced Mo. Stoichiometric amounts of these constituents and the Mo powder were then thoroughly ground together, densified into pellet form, and sintered at 1250 °C for 24 h. The resulting powder was reground, pressed, and sintered for an additional 24 h at 1250 °C to promote homogeneity. The nominal starting composition of the material was $Ho_{1.2}Mo_6S_8$; however there is no evidence in the crystal structure data, or in our own data, for more than one Ho ion per formula unit. We will therefore take the sample concentration to be the stoichiometric $HoMo_6S_8$. This consideration affects only the determination of the low-temperature saturated magnetic moment from the diffraction data. We will discuss this assumption further at that time.

For the diffraction data the sample was mounted in a dilution refrigerator with a low-temperature capability of ~50 mK. The incident neutron energy was 13.7 meV, and the horizontal collimation before and after the pyrolytic graphite monochromator and analyzer was varied between 10′ and 40′ full width at half maximum (FWHM) as dictated by intensity and resolution considerations. A pyrolytic graphite filter was used in the incident beam to reduce higher-order wavelength contaminations. For the study of the oscillatory magnetic phase a He^3 refrigerator was employed. Most of the small-angle scattering measurements in this case were made with an incident energy of 3.72 meV, with 10′ FWHM collimation before and after the sample. A cold Be filter was placed in the incident beam, and 40′ FWHM vertical collimation was placed before the detector to restrict the vertical divergence. An air-gap electromagnet was mounted on the outside of the cryostat with the field directed along the scattering vector. Only 400 Oe could be achieved in this configuration, but this was ample for our purposes.

Neutron-diffraction measurements at room temperature and 1.3 K confirmed that the crystal structure is rhombohedral ($R\bar{3}$), with one formula unit per unit cell.[15] The Ho ions in this structure occupy a simple primitive lattice which is nearly simple cubic since the rhombohedral angle is close to 90° in these materials. A least-squares refinement of the positions of eight peaks at 1.3 K yielded the lattice parameters shown in Table I. The lattice parameters at room temperature measured by both x rays and neutrons are also given in the table.

The positions of the Mo and S in the unit cell have been determined at room temperature by x-ray scattering.[16] Our neutron measurements of the intensities agreed well with calculations of the nuclear structure factors based on these positions. In particular the calculated {200} nuclear scattering is small, and no {200} peak was observed. This result provides a sensitive test of the validity of the crystal structure. We did not, however, have a sufficient data set to refine the positional parameters. There was also evidence of a small amount of unreacted Mo_2S_3 in the sample as well as an unidentified magnetic impurity phase (not HoS or Ho_2O_2S), but their presence is irrelevant to the behavior of $HoMo_6S_8$ as far as our neutron measurements are concerned.

Table I also gives the superconducting transition temperatures measured by ac susceptibility techniques[17] on the same sample used in the present neutron studies. The values for the reentrant transition are in good agreement with the results of Ishikawa and Fischer,[18] whereas the value of $T_{c1}=1.82$ K for the upper transition, while consistent with our earlier work,[19] is considerably higher than their value of $T_{c1}=1.25$ K. This difference is most likely due to differences in the sample preparation. For the reentrant transition there is a 56 mK difference between the curves on heating and cooling, whereas for the upper transition there is no observed hysteresis.

III. FERROMAGNETIC STATE

The temperature dependence of the {100} Chevrel phase peak is shown in Fig. 1. Above ~0.7 K the scattering is essentially independent of temperature and originates from the nuclear Bragg scattering, diffuse paramagnetic scattering, and background. Below

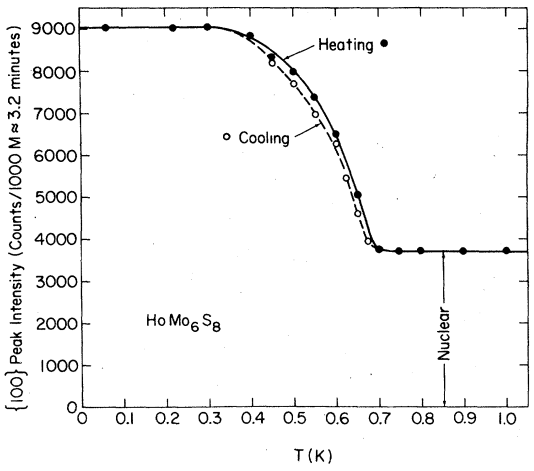

FIG. 1. Peak intensity of the {100} peak as a function of temperature. The intensity above T_M is due to the nuclear Bragg scattering, which is temperature independent. The additional intensity below $T_M \sim 0.67$ K is magnetic in origin and is proportional to the square of the order parameter. M represents monitor.

~ 0.7 K there is a rapid rise in the scattering which is associated with the development of magnetic order. The magnetic transition occurs at a temperature of $T_M \simeq 0.67$ K, which is close to the reentrant superconducting phase transition in this material. Furthermore we can conclude that the spin alignment is basically ferromagnetic in nature since the magnetic peak position coincides with the nuclear peak. We also note that there is a small difference in the data on warming and cooling, corrresponding to a temperature difference of about 15 mK. We will discuss this aspect of the scattering more thoroughly in the next section, where we will see that there is a marked difference between the behavior of the magnetism on warming and cooling in the vicinity of the reentrant superconducting transition.

To definitively characterize the magnetic state at low temperature, complete diffraction patterns were taken from 2 to 80° at several temperatures above and below the magnetic transition. Figure 2 shows the diffraction data at 50 mK. For convenience we have simply labeled the Chevrel phase peaks with cubic indices since the rhombohedral distortion is small in this system. The effect of this distortion is indicat-

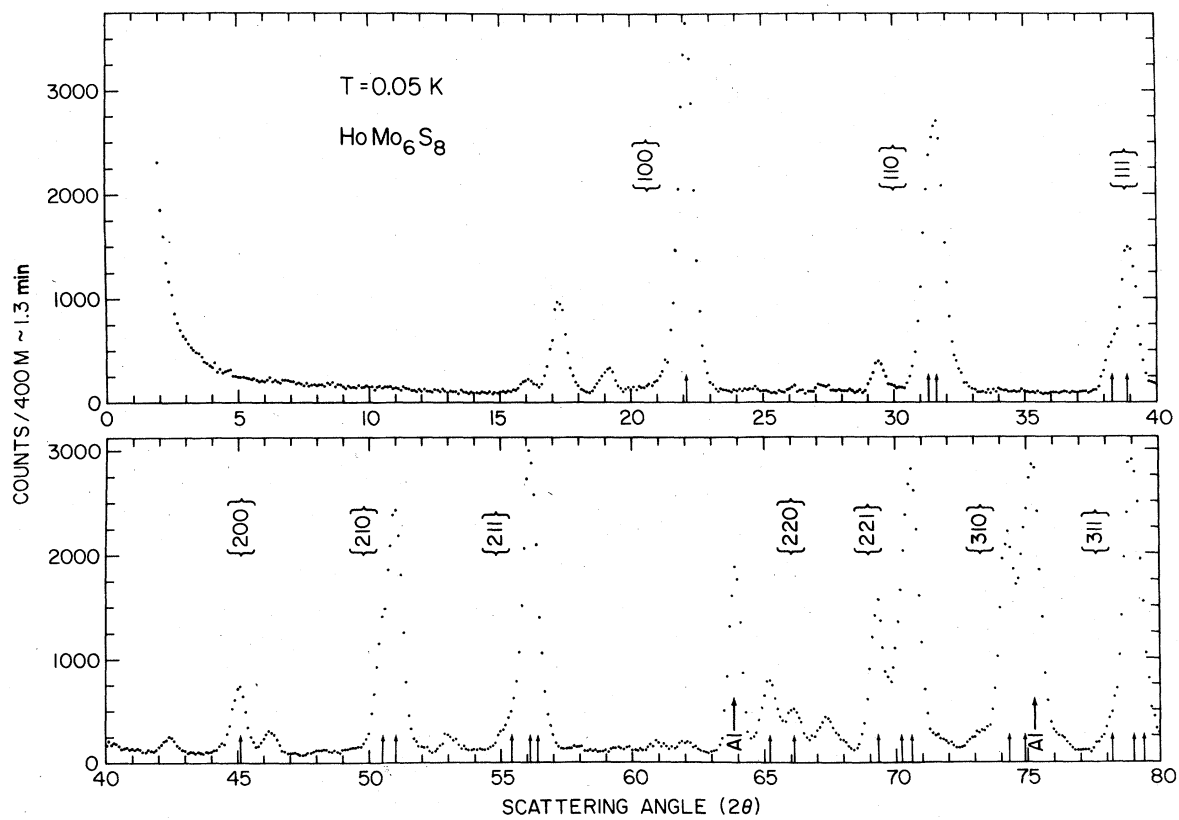

FIG. 2. Powder diffraction pattern for $HoMo_6S_8$ below the magnetic phase transition. The peaks are labeled by cubic indices for simplicity, since the rhombohedral angle is nearly 90°. The actual rhombohedral peak positions are shown by the arrows. M again represents monitor.

ed by the arrows which locate the "split" peak positions, which are resolved at the higher scattering angles. Note, for example, the separation of the {220} peak into the rhombohedral {220} peak at 65.2° and the $\{2\bar{2}0\}$ at 66.1°.

In addition to the peaks from the $HoMo_6S_8$, we also observed Bragg peaks which did not belong to the Chevrel phase. The peaks at 63.9° and 75.3°, for example, are aluminum peaks from the sample holder, but there are also additional small peaks originating from impurity phases in the sample as discussed earlier. These additional peaks have no temperature dependence in the region of interest, and we see in Fig. 3 that the difference between scans at 1.0 and 0.05 K yields a series of resolution limited peaks which are associated only with the Chevrel phase. The magnetic state at low temperature is thus ferromagnetic, and it is unambiguously associated with the $HoMo_6S_8$ Chevrel phase. The change in the apparent "background" away from the Bragg peaks is due to the absence of the diffuse paramagnetic scattering at low temperatures.

For a simple collinear magnetic structure the coherent magnetic cross section can be written as[20]

$$\left(\frac{d\sigma}{d\Omega}\right)_{\text{mag}} = \left(\frac{\gamma e^2}{2mc^2}\right)^2 \langle \mu_z \rangle^2 |\vec{f}(\vec{K})|^2 \langle 1 - (\hat{K}\cdot\hat{\eta})^2 \rangle \times \delta(\vec{K} - \vec{\tau}) \ , \quad (1)$$

where

$$\left(\frac{\gamma e^2}{2mc^2}\right) = -0.2695 \times 10^{-12} \quad (2)$$

(expressed in units of cm) is the neutron-electron magnetic dipole coupling constant, $\langle \mu_z \rangle$ is the average z component of the magnetic moment, $\vec{K}$ is the neutron momentum transfer, and $\hat{\eta}$ is a unit vector in the spin direction. Here $\vec{\tau}$ is a magnetic reciprocal-lattice vector, which for the ferromagnetic case of interest coincides with the chemical reciprocal-lattice vector. Finally $\vec{f}(\vec{K})$ is the magnetic form factor, which is the Fourier transform of the magnetization density. This magnetization density originates from the Ho^{3+} $4f$ electrons and from the supercurrents. Since the $4f$ electrons are highly localized, the form factor decreases slowly with increasing wave vector. The supercurrents, on the other hand, have a very large spatial extent so that the associated magnetic form factor will have an appreciable value only at small wave vectors. Thus at the ferromagnetic Bragg peaks only the Ho ions will contribute to the intensity, whereas at small scattering angles both the localized $4f$ moments and the superconducting electrons can contribute.

For powder data the observed intensity of each diffraction peak corresponds to a sum of intensities from all reciprocal-lattice vectors of the same length. In general information is lost in this average, and

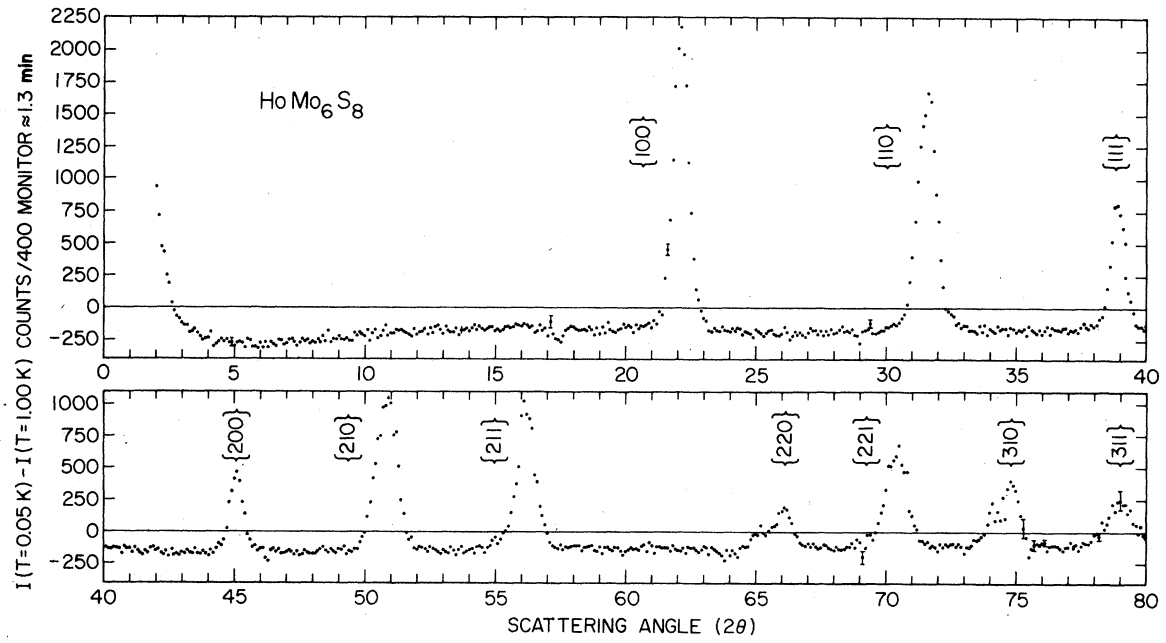

FIG. 3. Magnetic diffraction pattern obtained by subtracting the data taken at high temperature (1.0 K) from the data at 0.05 K. The new Bragg peak positions coincide with the $HoMo_6S_8$ nuclear peaks, establishing that the magnetic state corresponds to long-range ferromagnetic order.

thus single-crystal data may be needed in order to determine the spin direction $\hat{\eta}$. However, for a crystal structure which possesses a unique axis, powder data are sufficient to ascertain the angle between the spin direction and this unique axis.[21] For the Chevrel phase the [111] trigonal (rhombohedral) axis is unique. Thus to determine the spin direction, high-resolution scans of the (111) and (11$\bar{1}$) peaks were taken above and below T_M and are shown in Fig. 4. The subtraction of these data yields the magnetic contribution, and we see from Fig. 4(b) that there is no peak at the (111) position. From Eq. (1) we find that this necessarily implies that $\hat{\eta} \| (111)$, so that the magnetic moments are directed along the trigonal axis (at low temperatures). We are thus rather fortunate in this system that the magnetic structure can be completely determined from powder data alone, as there are no single crystals of sufficient size available yet for neutron studies.

Once the spin direction has been determined, Eq. (1) may be used to determine the magnetic form factor. Figure 5 shows the measured square of the form factor obtained from the diffraction data of Fig. 3

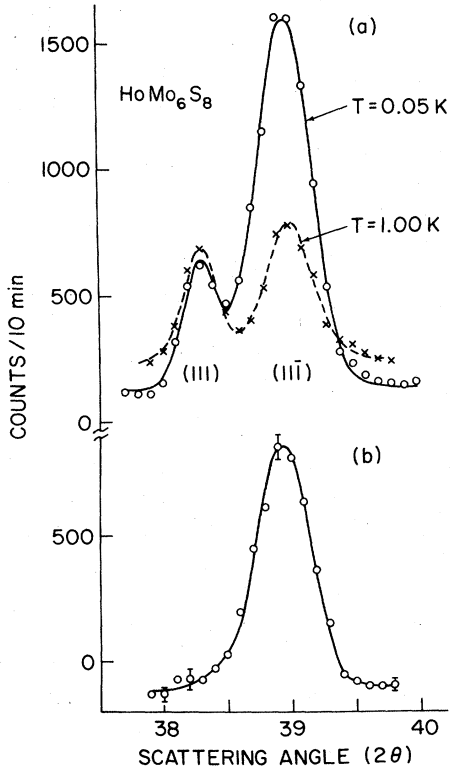

FIG. 4. (a) High-resolution scans of the (111) and (11$\bar{1}$) reflections above and below the transition. The difference between these two scans (b) shows that the magnetic contribution occurs only for the (11$\bar{1}$) reflection, so that the easy magnetic axis is the trigonal [111] direction.

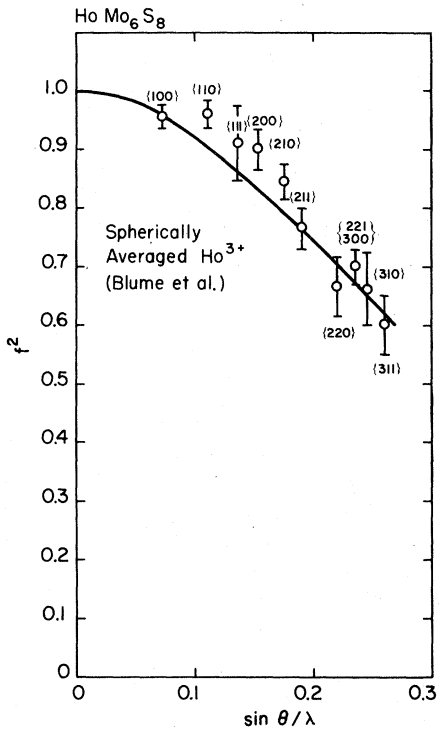

FIG. 5. Measured square of the magnetic form factor for $HoMo_6S_8$, showing that there is good agreement between theory and experiment assuming there is one Ho ion per unit cell with the spin direction along the [111] direction.

(note: $|\vec{K}|/4\pi = \sin\theta/\lambda$). The reciprocal-lattice points are designated by the cubic notation since we did not attempt to extract separate intensities from peaks which are split by the small trigonal distortion. The solid curve is the spherically averaged form factor calculated by Blume, Freeman, and Watson.[22] The error bars on the data correspond to one standard deviation due to statistical uncertainties, so that we conclude that there is good agreement between theory and experiment. We should remark here that these data do not represent a strong test of the theory; rather the point is that the data agree with the calculated magnetic form factor, so that the scattering is unambiguously magnetic in origin, and that a consistent set of data is obtained based on the assumption of one Ho ion per unit cell.

Finally we can put the magnetic intensities on an absolute basis by comparison with the nuclear intensities. The cross section for nuclear Bragg scattering is given by[20]

$$\left(\frac{d\sigma}{d\Omega}\right)_{\text{nuc}} = |F_N|^2 = \left|\sum_{j=1}^{N'} c_j b_j e^{i\vec{K}\cdot\vec{r}_j}\right|^2 , \qquad (3)$$

where F_N is the nuclear structure factor, b_j is the coherent nuclear scattering length, and c_j the occupancy probability for the jth atom located at $\vec{r}_j$, and

TABLE II. Magnetic moment per Ho ion measured by different techniques.

$\mu_z(\mu_B)$	Method	Reference
9.06±0.3	Neutron-diffraction low-temperature ferromagnetic phase	Present study
9.0±0.1	Neutron-diffraction-induced moment	Lynn and Shelton (Refs. 23 and 24)
9.91	Susceptibility	Pelizzone *et al.* (Ref. 25)
6.1	Low-temperature magnetization	Ishikawa and Muller (Ref. 26)

the sum is over all N' atoms in the unit cell. The b_j are known, so that if the coordinates $\vec{r}_j$ of the atoms have been determined from crystallographic studies then F_N can be calculated. We explicitly assume that all the c_j are unity. For any particular Bragg peak we then have

$$\frac{I_{\text{mag}}}{I_{\text{nuc}}} = \left(\frac{\gamma e^2}{2mc^2}\right)^2 \frac{\langle \mu_z \rangle^2 |\vec{f}(\vec{K})|^2 \langle 1-(\hat{\tau}\cdot\hat{\eta})^2 \rangle}{|F_N|^2} \tag{4}$$

and we see that the temperature dependence is proportional to the square of the magnetic moment μ_z. We emphasize that this is the z component of the magnetic moment, which for a free ion would be given by gJ, and not the "effective" moment $g\sqrt{J(J+1)}$.

For the crystallographic coordinates given by Yvon,[16] the {100} nuclear cross section is calculated to be 1.762 b. This in turn gives from Eq. (4) a value of $\mu_z f = (8.85 \pm 0.3)\mu_B$. The quoted error represents one standard deviation due to the statistical error and does not include estimates of possible systematic errors such as might be introduced through uncertainties in the nuclear structure factors. At small momentum transfers the aspherical contribution to the magnetic form factor is small, so to a very good approximation $f\{100\}$ is given by the spherically averaged value of 0.977. The resultant saturated magnetic moment is $\mu_z = 9.06\mu_B$ per formula unit, which is the value of the Ho moment assuming one holmium ion per unit cell. Comparisons with other determinations of the moment are given in Table II. The present determination is in very good agreement with the neutron determination at 5 K by inducing the moment with a magnetic field.[23,24] This induced moment value is also subject to the same assumptions concerning the nuclear structure factors; however, it does prove conclusively that the entire sample has ordered ferromagnetically at low temperature, independent of any assumptions about F_N. These values determined by neutron scattering are in reasonable agreement with susceptibility measurements,[25] but are substantially higher than the value determined by low-temperature magnetization measurements.[26] In the magnetization measurements, however, complete saturation was not observed. We remark that the neutrons directly measure the moment in the Chevrel phase material only, while bulk techniques will also be sensitive to magnetic impurity phases. A small concentration of a magnetic impurity phase has been observed in the neutron induced-moment studies[23,24] as well as in the present data.

One final point is that at these low temperatures the Ho nuclei will become aligned.[27] For an unpolarized neutron beam this will not affect the coherent nuclear scattering cross section, so that no effect will be found in the present measurements. For a polarized neutron beam, however, the nuclear Bragg cross section would be dependent on the degree of nuclear polarization since the nuclear force is spin dependent.

IV. FERROMAGNETIC CORRELATIONS AND THE OSCILLATORY STATE

As the magnetic phase transition is approached from high temperatures, spatial correlations between the Ho spins develop as evidenced by enhanced scattering at small wave vectors. Figure 6(a) shows[12] the temperature dependence of this scattering at a momentum transfer of 0.09 Å^{-1}, where the critical scattering peaks near the phase transition as would be expected for a conventional ferromagnetic phase transition. We also note that there is a large intensity at low temperatures, which is clearly not due to critical scattering. This scattering is present in all our measurements at low temperatures, and it is not particularly sensitive to the application of a modest magnetic field. The origin of this scattering is most likely from domain walls, which have been seen in other ferromagnets such as EuO and EuS (Ref. 28) as well as ferroelectrics such as lead germanate.[29] High-resolution measurements capable of probing smaller wave vectors would be most useful in unambiguously establishing the nature of this scattering.

For the usual ferromagnetic phase transition the wave-vector-dependent correlation function is of the

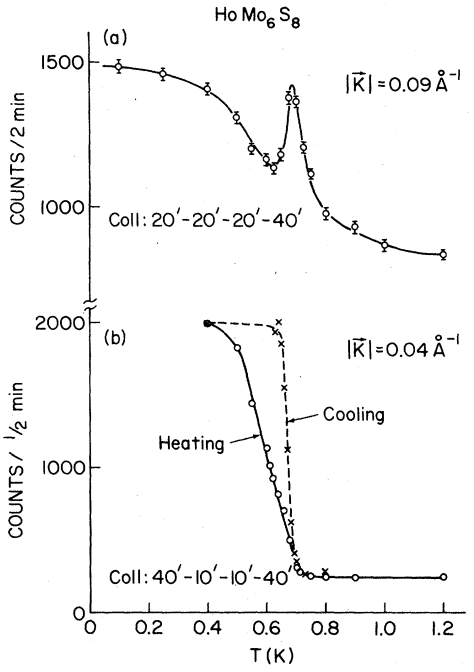

FIG. 6. Temperature dependence of the small-angle scattering. At a wave vector of 0.09 Å^{-1} there is a component to the scattering which peaks at the transition as expected for a ferromagnetic transition. At 0.04 Å^{-1} we see quite a different behavior to the scattering, which is strongly dependent on whether the data are taken on heating or cooling. The curves are simply guides to the eye.

Ornstein-Zernike form[20]:

$$\frac{d\sigma}{d\Omega} \propto \frac{1}{|\vec{K}|^2+\kappa^2} , \tag{5}$$

where κ is the inverse of the correlation range ξ in real space ($\xi = 1/\kappa$). Since the magnetic energy in this system is very small compared to the instrumental resolution, we effectively integrate in our measurements over the fluctuation spectrum. We may then compare our data directly by convoluting Eq. (5) with the wave-vector resolution of the instrument. At each temperature we have done a least-squares fit with κ treated as a free parameter. For $T > 0.69$ K relatively good fits to the data could be achieved, with ξ increasing steadily with decreasing temperature. At $T = 0.69$ K we obtained $\xi = 19$ Å. We may thus conclude that ferromagnetic corrrelations develop while the material is still in the superconducting state. Below 0.69 K, however, Eq. (5) did not adequately represent the data, with the fit being particularly poor at smaller wave vectors ($|\vec{K}| < 0.05$ Å^{-1}). Experimentally this is because there is more observed intensity at small wave vectors than expected on the basis of Eq. (5). Figure 6(b) shows indeed that the scattering at small wave vectors undergoes a dramatic increase of intensity below 0.69 K. Moreover the strength of this scattering depends very markedly on whether we are on a warming cycle or cooling cycle.

To investigate the origin of this scattering higher resolution measurements were taken at small angles. Figure 7 shows the observed scattering as a function of wave vector for several temperatures, after subtracting the background scattering measured at 1.3 K. At 0.7 K we begin to detect scattering which has a *maximum at a finite wave vector,* and this scattering grows rapidly in intensity with decreasing temperature. The observed peak at a wave vector of ~ 0.025 Å^{-1} corresponds (after correction for instrumental resolution) to a wavelength in real space of ~ 230 Å. The measured reentrant transition temperature for this sample is 0.612 K on cooling, so that it is most definitely still superconducting.

The nature of this scattering is fundamentally different from that expected for a conventional second-order ferromagnetic transition. Equation (5) shows that at each temperature the intensity is maximum at $\vec{K} = 0$ and monotonically falls toward zero with increasing $|\vec{K}|$. The overall strength of the scattering increases as T_M is approached, and in fact the scattering diverges at $\vec{K} = 0$, $T = T_M$, a characteristic feature of a ferromagnetic phase transition. For a coupled ferromagnetic superconductor, on the other hand, one can argue on rather general grounds[30–36] that the

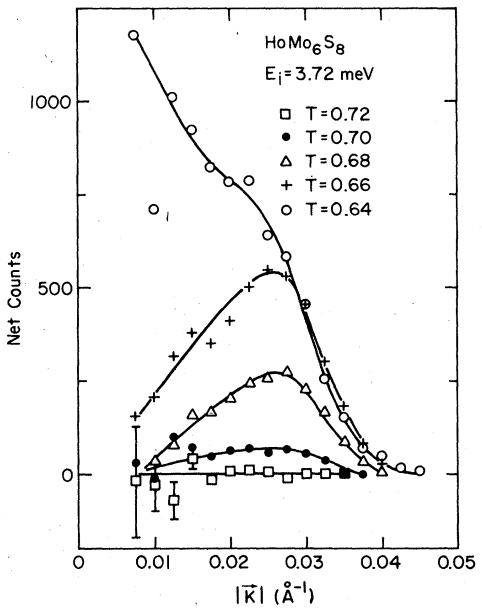

FIG. 7. High-resolution measurements of the small-angle scattering in the vicinity of the reentrant transition, showing that upon cooling a peak in the scattering intensity vs wave vector develops at ~ 0.027 Å^{-1}. This corresponds to an oscillatory magnetization in the system with a wavelength of ~ 230 Å.

long-wavelength (small $|\vec{K}|$) magnetic fluctuations will be energetically costly for the superconductor, and consequently they will be relatively unlikely compared to the short-wavelength fluctuations. We might then expect that Eq. (5) will be modified so that a maximum will occur at some finite wave vector. If long-range order is established then there will be a Bragg peak at this wave vector $\vec{\delta}$, and the reduced wave vector of the fluctuation spectrum should be taken as $\vec{K}-\vec{\delta}$ rather than $\vec{K}$ itself.

The assumption of long-range order yields a good representation of the data for $T > 0.66$ K, and the solid curves in Fig. 7 are the result of a least-squares fit of a δ function convoluted with the instrumental resolution (the curve for $T = 0.64$ K is simply a "guide to the eye"). The asymmetric shape of the curve is due primarily to the vertical divergence, which contributes substantially to the resolution at these small wave vectors. The resulting value for $\delta = (0.0275 \pm 0.005)$ Å^{-1}, which corresponds to a wavelength of $\sim (230 \pm 50$ Å). The relatively large uncertainty[37] is due to the difficulty of the experiment, as can be appreciated by noting the error bars in Fig. 7. They are shown only for $T = 0.72$ K, but are essentially the same for all the other sets of data shown. The rapid increase in the error bars at small K is due to the rapid increase in the background scattering caused by the incident beam ($K = 0$), which prohibited the collection of useful data below $K \approx 0.0075$ Å^{-1}.

The temperature dependence of the intensity of the scattering at a wave vector near the maximum is shown in Fig. 8. With no magnetic field applied, this oscillatory magnetization rapidly develops on cooling and reaches a maximum at $T \simeq 0.65$ K. The reduction in intensity at lower temperatures coincides with the temperature region where the bulk susceptibility measurements begin to show a return to the normal state. The measured width of the superconducting transition is ± 34 mK (see Table I) with the center at 0.612 K on cooling. In this same temperature range the neutron results reveal that the oscillatory state is only metastable. For example if the sample is cooled quickly from the superconducting state to 0.62 K, the intensity at this wave vector rapidly increases to twice the peak value shown in Fig. 8, and then slowly decreases to ~ 360 counts/min over a period of about an hour. At higher temperatures the oscillatory state is stable at least for a time scale of days. There is substantial scattering remaining at low temperatures as has been noted earlier in the discussion of Fig. 6. We have also noted that at 0.690 and 0.635 K the time needed for the system to come into thermal equilibrium was about five times longer than at all the other temperatures.

The evolution of the scattering from low temperatures is quite different. The scattering monotonically falls to zero with increasing temperature with no indication of the oscillatory magnetization. There is also no peak at finite wave vector as evidenced from the data of Fig. 9. There is, however, a considerable amount of small-angle scattering, which could be due to "domain wall scattering," or to an oscillatory peak at a smaller wave vector. We can say definitely that the wavelength λ of such an oscillation, if it exists, must exceed ~ 800 Å.

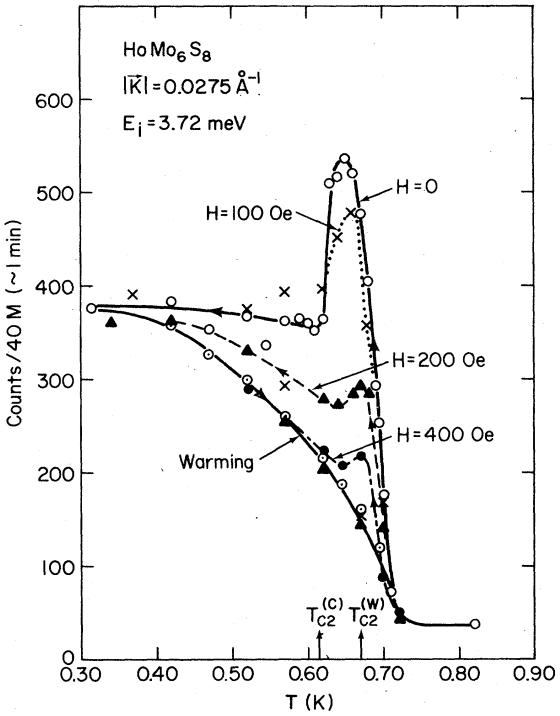

FIG. 8. Temperature dependence of the scattering at a wave vector of 0.0275 Å^{-1}. On cooling the intensity increases rapidly as the oscillatory state develops, then decreases as ferromagnetism sets in and the superconductivity is destroyed. An applied field is seen to suppress the oscillatory state (at this wave vector), and no oscillatory state is observed on warming. The reentrant superconducting transition temperatures on cooling (C) and warming (W) are indicated at the bottom. The curves are simply guides to the eye.

The oscillatory magnetization is affected markedly by an applied magnetic field. We see in Fig. 8 that the intensity at 0.0275 Å^{-1} decreases rapidly with increasing field, and extrapolation to higher fields suggests that for $H > \sim 500$ Oe the scattering would follow a single reversible curve on warming and cooling. We also note that the field has little effect on the "domain wall scattering" at low temperatures. Figure 10 shows that the principal effect of the magnetic field is in fact to shift the scattering to *smaller* wave vectors. This corresponds to an increase in the wavelength of the oscillation in real space toward the

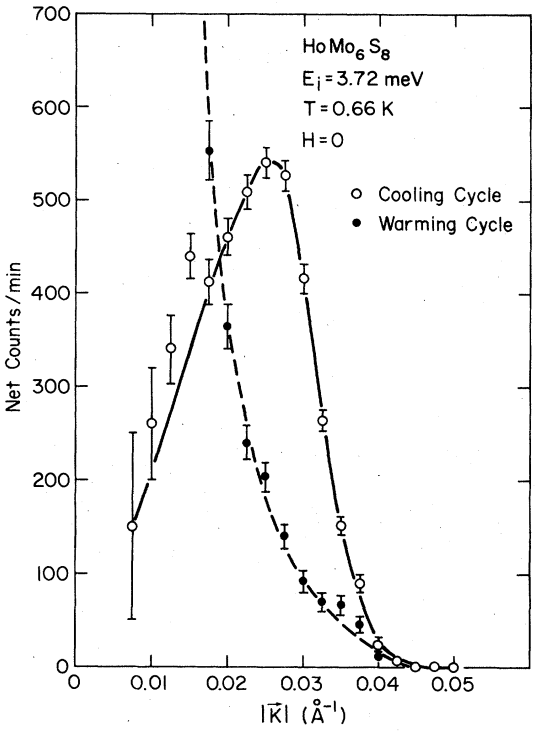

FIG. 9. Scattering intensity as a function of wave vector at a temperature of 0.66 K, showing that no oscillatory state is observed on warming. At this temperature the sample is superconducting on the cooling cycle, but not on the warming cycle.

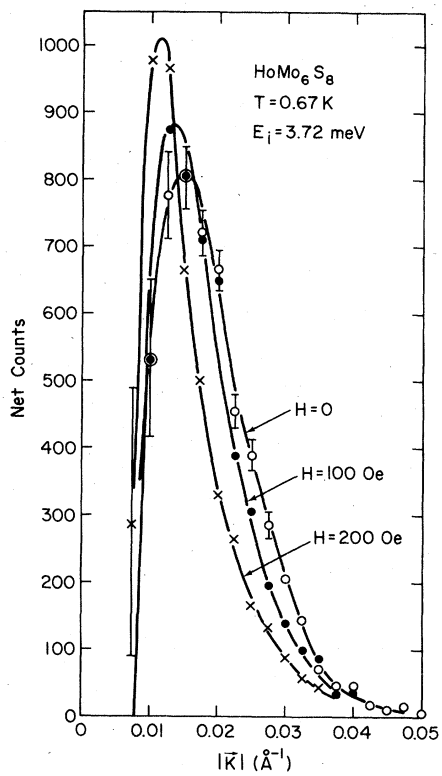

FIG. 10. Scattering as a function of wave vector at several fields, showing that the intensity shifts to smaller wave vectors with increasing field. Thus with the aid of a field the wavelength of the oscillation increases toward the ferromagnetic limit $\lambda = \infty$.

ferromagnetic limit ($\lambda = \infty$). The magnetic field is also found to be detrimental to the superconducting state, but 300 Oe is not sufficient to completely destroy the superconductivity.[18]

We have also been able to observe the effects of the oscillatory state around the {100} powder Bragg peak. Figure 11(a) shows the net intensity distribution observed upon cooling to 0.68 K after subtraction of the scattering at 1.0 K. For comparison the peak intensity of the {100} nuclear peak was 7678 counts/10 min, and its position is indicated by the arrow at the bottom of the figure. In zero field there are two peaks present on either side of a central component whose position coincides with the nuclear peak position. It should be kept in mind that the central component here does not necessarily imply that there is a ferromagnetic component. (It would, however, if there were a central component at *all* peak positions such as in Fig. 3.) In a powder we can only measure the projection of $\vec{\delta}$ perpendicular to the powder ring, i.e., we can only measure the *length* of $\vec{\tau} \pm \vec{\delta}$. For example if $\vec{\delta}$ were along the [100] direction, then we would have the possibilities $(1 \pm \delta, 0, 0)$, $(1, \pm\delta, 0)$, and $(1, 0, \pm\delta)$ (and cyclic permutations). The combinations $1 \pm \delta$ will give d spacings on either side of the {100} peak, as $\vec{\delta}$ is parallel to $\vec{\tau}$. The other four peaks have essentially the same d spacing as the nuclear peak since $\vec{\delta} \perp \vec{\tau}$ with $|\vec{\delta}| << |\vec{\tau}|$. This example will certainly give a three-peaked structure. The solid curves in Fig. 11(a) are in fact the result of a least-squares fit of three Gaussian peaks whose widths were fixed to the instrumental (Gaussian) width. The resulting value for δ in this case is 0.0166 Å^{-1}, which is considerably smaller than the value found from the data of Fig. 7. A more compatible value can be obtained if we assume that $\vec{\delta}$ is along the unique [111] direction, which then gives $\delta = \sqrt{3} \times 0.0166 = 0.0287$ Å^{-1} (see also Ref. 37). However, this assumption would produce only side peaks with no peak in the center. Thus $\vec{\delta} \parallel [111]$ could only be consistent with the data if there were in addition a ferromagnetic component of the magnetization. The possibility of a macroscopic magnetization *coexisting with superconductivity* cannot be ruled out experimentally at this time.

Figure 11(b) shows the effect a magnetic field has on this scattering. These data were obtained by cooling to 0.68 K in a field of 300 Oe, and then subtracting the data obtained by cooling in zero field. The

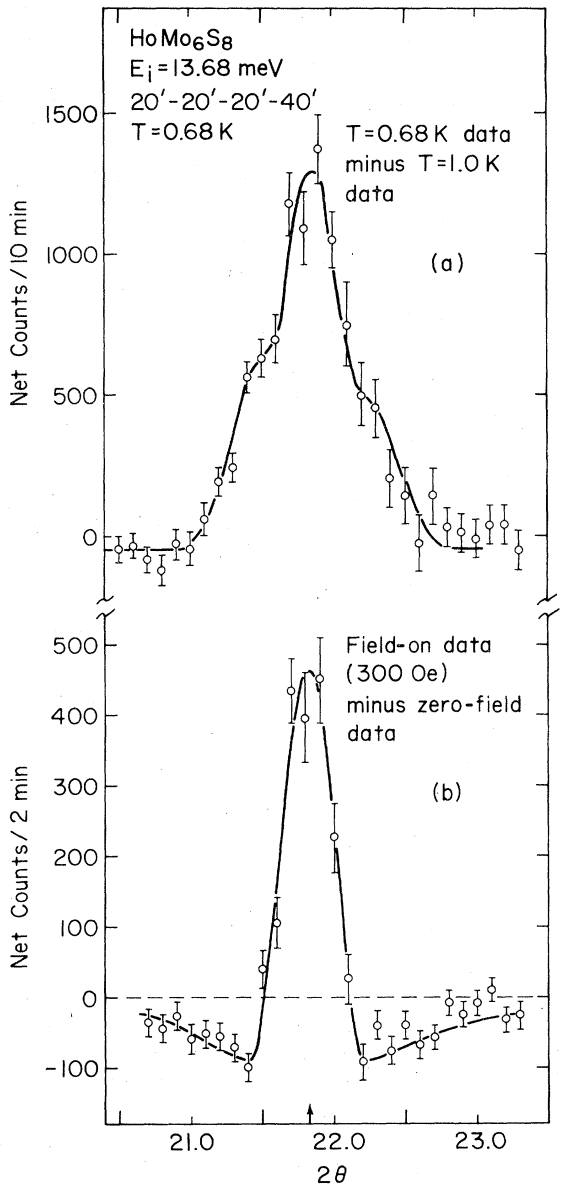

FIG. 11. Observed scattering around the {100} Bragg position (indicated by the arrow), showing the effect of the oscillatory state on the magnetic scattering at 0.68 K. (a) The difference between the scattering at 0.68 K and the nuclear-only scattering at 1.0 K. (b) The difference between field-on and zero field, showing that the side peaks found in (a) shift to coincide with the nuclear position (i.e., ferromagnetic alignment) when the field is applied.

effect of the magnetic field is to make $|\vec{\delta}|$ smaller, so there is a loss of intensity where the side peaks used to be and an increase of intensity at the central position. These data also reveal that 300 Oe is not sufficient to align the magnetic moments along the field direction, since if alignment were achieved then $\hat{\kappa}\cdot\hat{\eta}=1$ and the intensity would vanish [see Eq. (1)]. An analogous argument shows that the oscillatory state must also be transversely polarized to be observed around the forward direction. We believe these data around the {100} peak provide strong evidence that the oscillatory state is in reality long range in character, as diffuse critical scattering with a peak at finite wave vector, after doing a powder average, would not yield the structure observed. Our best estimate for the lower limit of the coherence length for the oscillatory state is ~ 1500 Å, or about six periods.

For the ferromagnetic case the widths of the peaks are also resolution limited. If we assume no transition has actually occurred, but rather an intrinsic breadth to the critical scattering is hidden in our resolution, then we obtain from Eq. (5) a lower limit of ~ 300 Å to the correlation range ξ. Alternatively, if the scattering were actually oscillatory ($\delta \neq 0$) rather than ferromagnetic but with a δ too small to produce any breadth to the peak, then the estimated minimum wavelength would be $\sim 10^3$ Å.

V. DISCUSSION

In these magnetic-superconductor materials the Abrikosov-Gorkov spin-depairing mechanism is not effective in destroying the superconductivity because of the effective isolation of the rare-earth ions from the superconducting electrons. This is certainly a necessary condition for the presence of superconductivity in these magnetic systems. If the magnetic system prefers to order as a compensated antiferromagnet then there is no macroscopic magnetic field associated with the magnetic order and consequently no strong interaction with the superconductivity. There are now in fact a rather large number of examples of antiferromagnetic superconductors.[10]

The behavior in the case of ferromagnetic alignment may be quite different since the macroscopic dipolar field associated with this system should perturb the superconducting state in a fashion similar to an externally applied field. To understand qualitatively the nature of the competition between these two cooperative phenomena, we note that above the magnetic ordering temperature T_M the long-wavelength fluctuations for an unperturbed ferromagnet are energetically the most favorable and thus they dominate the spectrum as in Eq. (5). The response of the superconductor to these fluctuations will depend on their wavelength; if the wavelength is less than some characteristic length λ (which in the local approximation is the London penetration depth) then the response will be weak; while if the wavelength is long compared to λ the response will be strong. The essential point is that the magnetic fluctuations which are energetically the most favorable for ferromagne-

tism are the most unfavorable for superconductivity. This should result in a maximum in $\chi(|\vec{K}|)$ at finite $|\vec{K}|$, which at lower temperatures may trigger a phase transition to an oscillatory magnetic state rather than a transition to a conventional uniform ferromagnetic state.

A number of calculations have appeared recently which predict the possibility of a nonuniform "ferromagnetic" state.[30–36] Blount and Varma[31] point out that electromagnetic effects should dominate the energetics in these low T_M systems. Using a Ginzburg-Landau (GL) approach they find that depending on the value of the parameters there is either a transition to a uniform ferromagnetic state along with a reentrance to the normal conducting state, or that an oscillatory state forms in the superconductor. In either case they expect the precursor critical scattering to have a peak at finite $|\vec{K}|$. Kuper *et al.*[35] have found using a very similar GL approach that the lowest energy state may correspond to the formation of a spontaneous vortex lattice, and a spontaneous vortex lattice has also been anticipated by Tachiki *et al.*[33] Ferrell *et al.*[32] have used an approach to the spin-spin correlation problem which emphasizes the importance of nonlocality in calculating the diamagnetic response of the superconducting electrons, as well as the modification to the Ruderman-Kittel-Kasuya-Yosida (RKKY) exchange interaction. The change in the RKKY interaction is what led Anderson and Suhl[30] to propose the "cryptoferromagnetic" state. In the present case, however, the effect on the exchange interaction should be small in comparison to the electromagnetic effects.

For $HoMo_6S_8$ the observed peak in the scattering most likely corresponds to an oscillatory state of long-range order. This statement is based on the fact that the width of the oscillatory scattering is resolution limited, because of the strength of the oscillatory scattering and the rapid development of the intensity on cooling, and because we observe a rather long time constant for the system to come into equilibrium upon entering and upon exiting the temperature region where the oscillatory scattering is found. According to theory[31] this oscillatory scattering could originate from either a spiral (S) state, a linearly polarized (LP) state, or to the spontaneous formation of a vortex lattice. The (S) and (LP) states are both transversely polarized, consistent with our observations, but our data do not allow a choice between them. Neither state possesses a ferromagnetic component, and one of the unresolved questions is whether there is a ferromagnetic component experimentally. We can say, though, that the scattering is likely not due to the formation of a vortex lattice, since the scattering shifts to smaller $|\vec{K}|$ with field. The spacing between vortices would be expected to *decrease* with increasing field as more vortices are formed in the lattice, and thus the scattering peak would be expected to move to larger $|\vec{K}|$.[38] We remark that the oscillatory magnetic scattering observed around the {100} Bragg peak must originate solely from the Ho ions since the magnetic form factor for the supercurrents is vanishingly small at any finite reciprocal-lattice point.

Finally we briefly compare the present results on $HoMo_6S_8$ with the behavior of the other known "ferromagnetic-superconductor" systems[39] $(Er_{1-x}Ho_x)Rh_4B_4$, $(Ce_{1-x}R_x)Ru_2$, and $ErRh_{1.1}Sn_{3.6}$. $ErRh_4B_4$ is the most closely related in that it is a reentrant ferromagnetic-superconductor[40,41] and there is a peak in the precursor scattering[11] at 0.06 Å^{-1}. According to Ginzburg-Landau theory[31] the wavelength of the oscillation is of order $(\gamma\lambda)^{1/2}$, where γ is the magnetic stiffness and λ is the London penetration depth. Since the observed magnetic transitions are roughly comparable in temperature for $ErRh_4B_4$ and $HoMo_6S_8$ the γ's should be nearly equal, so that the penetration depth for $HoMo_6S_8$ should be $\sim$ four times that for $ErRh_4B_4$. These two materials differ further in that the strength of the oscillatory scattering for the $ErRh_4B_4$ is considerably less than expected for a long-range ordered state. Recent measurements[42] on a single crystal of $ErRh_4B_4$ are beginning to provide new details about the magnetic behavior of this system.

Preliminary results on a new system, $ErRh_{1.1}Sn_{3.6}$, show a reentrant superconducting phenomenon associated with the ferromagnetic alignment.[43] In this case, however, the widths of the "Bragg peaks" are quite broad indicating the ordering is not truly long range in nature. A similar situation occurs in the substitutional alloy system $(Ce_{1-x}R_x)Ru_2$, where ferromagnetic correlations develop in the superconducting state, but long-range ferromagnetic order does not appear except at high concentrations where the superconducting state is absent.[4–6,44]

VI. SUMMARY

Our neutron scattering and susceptibility measurements show that $HoMo_6S_8$ exhibits a number of phase transitions at low temperatures. Upon cooling the system first becomes superconducting at a temperature of $T_{c1} = 1.82$ K, then forms an oscillatory magnetic state with $\lambda = (230 \pm 50)$ Å while remaining superconducting. The sample reenters the normal conducting state at $T_{c2}^{(C)} = 0.612$ K, where the magnetic state appears to become purely ferromagnetic in nature. At low temperatures the ferromagnetic state is characterized by a moment μ_z per Ho ion of $(9.06 \pm 0.3)\mu_B$, with the spins parallel to the unique rhombohedral axis. On warming from low temperatures the oscillatory state appears to be bypassed, and the system transforms directly from the ferromagnetic state to the superconducting state at $T_{c2}^{(W)} = 0.668$

K. With continued increase of temperature the sample becomes normal again at the same temperature T_{c1} of 1.82 K.

The formation of the oscillatory state is a direct consequence of the competition between the ferromagnetism and superconductivity. Since these data were obtained on powder specimens it was not possible to unambiguously determine the crystallographic direction of the oscillatory wave vector, but the results are consistent with $\vec{\delta}$ along the unique [111] axis *if* there is a ferromagnetic component of the magnetization. Whether or not there is a net macroscopic magnetization in the superconducting-oscillatory state is certainly one of the interesting experimental questions to be resolved. The spiral and linearly polarized states which have been proposed theoretically do not have a ferromagnetic component, whereas the vortex solution does. However, experimentally we find that the oscillatory wave vector decreases in magnitude with increasing applied magnetic field, while the opposite behavior would be expected for the usual vortex lattice.

ACKNOWLEDGMENTS

We would like to thank J. Bhattacharjee, R. A. Ferrell, and C. M. Varma for helpful discussions, and H. C. Hamaker for carrying out one set of susceptibility measurements. Work at Maryland supported by the NSF Grant No. DMR 79-00908, and the Computer Science Center. Work at Brookhaven supported by the Division of Basic Energy Studies, DOE, under Contract No. DE-AC02-7c-CH00016. Work at Ames supported by the Director for Energy Research, Office of Basic Energy Sciences, WPAS-KC-02-02-02.

[1]B. T. Matthias, H. Suhl, and E. Corenzwit, Phys. Rev. Lett. 1, 449 (1958).
[2]M. Wilhelm and B. Hillenbrand, Z. Naturforsch. Teil A 26, 141 (1971); J. Phys. Chem. Solids 31, 559 (1970).
[3]See, for example, *Magnetism,* edited by G. T. Rado and H. Suhl (Academic, New York, 1966), Vol. V, Chaps. 10–12.
[4]S. Roth, Appl. Phys. 15, 1 (1978).
[5]J. W. Lynn, D. E. Moncton, L. Passell, and W. Thomlinson, Phys. Rev. B 21, 70 (1980).
[6]J. A. Fernandez-Baca and J. W. Lynn, J. Appl. Phys. 52, 2183 (1981).
[7]Ø. Fischer, Appl. Phys. 16, 1 (1978).
[8]For recent results see *Ternary Superconductors,* edited by G. Shenoy, B. Dunlap, and F. Fradin (North-Holland, New York, 1981).
[9]A. A. Abrikosov and L. P. Gorkov, Zh. Eksp. Teor. Fiz. 39, 1781 (1960) [Sov. Phys. JETP 12, 1243 (1961)].
[10]See the reviews by D. E. Moncton, G. Shirane, and W. Thomlinson, J. Magn. Magn. Mater. 14, 172 (1979); W. Thomlinson, G. Shirane, J. W. Lynn, and D. E. Moncton, *Topics in Current Physics* (in press).
[11]D. E. Moncton, D. B. McWhan, P. H. Schmidt, G. Shirane, W. Thomlinson, M. B. Maple, H. B. MacKay, L. D. Woolf, Z. Fisk, and D. C. Johnston, Phys. Rev. Lett. 45, 2060 (1980).
[12]J. W. Lynn, D. E. Moncton, W. Thomlinson, G. Shirane, and R. N. Shelton, Solid State Commun. 26, 492 (1978).
[13]J. W. Lynn, G. Shirane, W. Thomlinson, and R. N. Shelton, Phys. Rev. Lett. 46, 368 (1981).
[14]R. de Jonge, T. J. A. Popma, G. A. Wiegers, and F. Jellinek, J. Solid State Chem. 2, 188 (1970).
[15]M. Marezio, P. D. Dernier, J. P. Remeika, E. Corenzwit, and B. T. Matthias, Mater. Res. Bull. 8, 657 (1973).
[16]K. Yvon, in *Current Topics in Materials Science,* edited by E. Kaldis (North-Holland, New York, 1978), Chap. 2.
[17]L. D. Woolf, M. Tovar, H. C. Hamaker, and M. B. Maple, Phys. Lett. 71A, 137 (1979).
[18]M. Ishikawa and Ø. Fischer, Solid State Commun. 23, 37 (1977).
[19]R. N. Shelton, in *Superconductivity in d- and f-Band Metals,* edited by D. H. Douglass (Rochester, New York, 1970), pp. 137–160.
[20]W. Marshall and S. W. Lovesey, *Theory of Thermal Neutron Scattering* (Oxford, London, 1971).
[21]G. Shirane, Acta. Crystallogr. 12, 282 (1959).
[22]M. Blume, A. J. Freeman, and R. E. Watson, J. Chem. Phys. 37, 1245 (1962); 41, 1878 (1964).
[23]J. W. Lynn and R. N. Shelton, J. Magn. Magn. Mater. 18, 1577 (1980); J. Appl. Phys. 50, 1984 (1979).
[24]J. W. Lynn, in *Crystalline Electric Field and Structural Effects in f-electron Systems,* edited by J. Crow, R. Guertin, and T. Mihalisin (Plenum, New York, 1980), p. 547.
[25]M. Pelizzone, A. Treyvaud, P. Spitzli, and Ø. Fischer, J. Low Temp. Phys. 29, 453 (1977).
[26]M. Ishikawa and J. Muller, Solid State Commun. 27, 761 (1978).
[27]H. Marshak and B. G. Turrell, Solid State Commun. 30, 677 (1979).
[28]O. W. Dietrich, J. Als-Nielsen, and L. Passell, Phys. Rev. B 14, 4908 (1976).
[29]R. A. Cowley, J. D. Axe, and M. Iizumi, Phys. Rev. Lett. 36, 806 (1976).
[30]P. W. Anderson and H. Suhl, Phys. Rev. 116, 898 (1959).
[31]E. I. Blount and C. M. Varma, Phys. Rev. Lett. 42, 1079 (1979); Phys. Rev. B 22, 3507 (1980); C. M. Varma, in *Superconductivity in d- and f-Band Metals,* edited by H. Suhl and M. B. Maple (Academic, New York, 1980); C. M. Varma, E. I. Blount, H. S. Greenside, and T. V. Ramakrishnan, in *Ternary Superconductors,* edited by G. Shenoy, B. Dunlap, and F. Fradin (North-Holland, New York, 1981); H. S. Greenside, E. I. Blount, and C. M. Varma, Phys. Rev. Lett. 46, 49 (1981).
[32]R. A. Ferrell, J. K. Bhattacharjee, and A. Bagchi, Phys. Rev. Lett. 43, 154 (1979).
[33]M. Tachiki, H. Matsumoto, and H. Umezawa, Phys. Rev. B 20, 1915 (1979); Solid State Commun. 31, 157 (1979); M. Tachiki, A. Kotani, H. Matsumoto, and H. Umezawa, *ibid.* 31, 927 (1979); S. Maekawa, M. Tachiki, and S. Takahashi, J. Magn. Magn. Mater. 13, 324 (1979); S. Maekawa and M. Tachiki, Phys. Rev. B 18, 4688 (1978);

M. Tachiki, H. Matsumoto, T. Koyama, and H. Umezawa, Solid State Commun. 34, 19 (1980).
[34]M. V. Jaric and M. Belic, Phys. Rev. Lett. 42, 1015 (1979); M. V. Jaric, Phys. Rev. B 20, 4486 (1979); 22, 3503 (1980).
[35]C. G. Kuper, M. Revzen, and A. Ron, Phys. Rev. Lett. 44, 1545 (1980); Solid State Commun. 36, 533 (1980).
[36]T. K. Lee, V. Izyumov, and J. L. Birman, Phys. Rev. B 20, 4494 (1979); L. N. Bulaevskii, A. I. Rusinov, and M. Kulic, J. Low Temp. Phys. 39, 255 (1980).
[37]Recent higher-resolution measurements give $\delta = (0.030 \pm 0.001)$ Å^{-1}, J. W. Lynn, J. L. Ragazzoni, R. Pynn, and J. Joffrin, J. Phys. (Paris) Lett. 42, L45 (1981).
[38]See, for example, D. K. Christen, H. R. Kerchner, S. T. Sekula, and P. Thorel, Phys. Rev. B 21, 102 (1980).
[39]For a recent review see J. W. Lynn, in *Ternary Superconductors*, edited by G. Shenoy, B. Dunlap, and F. Fradin (North-Holland, New York, 1981), p. 51.
[40]W. A. Fertig, D. C. Johnston, L. E. DeLong, R. W. McCallum, M. B. Maple, and B. T. Matthias, Phys. Rev. Lett. 38, 987 (1977).
[41]D. E. Moncton, D. B. McWhan, J. Eckert, G. Shirane, and W. Thomlinson, Phys. Rev. Lett. 39, 1164 (1977).
[42]S. K. Sinha, H. A. Mook, D. G. Hinks, and G. W. Crabtree, Bull Am. Phys. Soc. 26, 277 (1981).
[43]J. P. Remeika, G. P. Espinosa, A. S. Cooper, H. Barz, J. M. Rowell, D. B. McWhan, J. M. Vandenberg, D. E. Moncton, Z. Fisk, L. D. Woolf, H. C. Hamaker, M. B. Maple, G. Shirane, and W. Thomlinson, Solid State Commun. 34, 923 (1980).
[44]J. W. Lynn and C. J. Glinka, J. Magn. Magn. Mater. 14, 179 (1979).